

Temperature dependence of narrow-band terahertz generation from periodically poled lithium niobate

Y.-S. Lee,^{a)} T. Meade, M. DeCamp, and T. B. Norris

Center for Ultrafast Optical Science, The University of Michigan, Ann Arbor, Michigan 48109-2099

A. Galvanauskas

IMRA America, 1044 Woodridge Avenue, Ann Arbor, Michigan 48105

(Received 12 May 2000; accepted for publication 5 July 2000)

Femtosecond optical pulses are used to generate narrow-band terahertz wave forms via optical rectification in a periodically poled lithium niobate crystal. By cooling the crystal to reduce losses due to phonon absorption, we are able to obtain bandwidths as narrow as 18 GHz at a carrier frequency of 1.8 THz. Temperature-dependent measurements show insignificant bandwidth broadening between 10 and 120 K, although the terahertz power substantially decreases as the temperature increases. Absolute power measurements indicate a conversion efficiency of at least 10^{-5} . © 2000 American Institute of Physics. [S0003-6951(00)01735-6]

Coherent terahertz (THz) radiation is of great interest in fundamental and applied sciences because many material excitations in molecular and condensed matter systems fall into the THz frequency range. Coherent THz can be applied to spectroscopy, sensing, communication, and imaging. For many applications, narrow-band THz sources are required. A number of approaches have therefore been taken to generate narrow-band THz radiation. These include difference-frequency generation,¹⁻³ photomixing,⁴⁻⁶ and optical parametric oscillation.⁷⁻⁹

The various techniques have a number of pros and cons. Difference frequency generation is easy to implement, but it has very poor conversion efficiency. Photomixing is quite suitable for very narrow band THz generation, but suffers from a narrow tuning range and the efficiency drops very fast above ~ 1 THz. Optical parametric oscillation (OPO) has a better conversion efficiency, but the tuning range has been limited to about 0.9–2.2 THz and it has proved difficult to get the bandwidth narrower than ~ 50 GHz. Additionally, OPO alignment can be difficult.

Recently, we have demonstrated a simple technique to generate narrow-band THz radiation.¹⁰ Femtosecond optical pulses are propagated through a periodically poled lithium niobate (PPLN) crystal, where the domain width is matched to the walk-off length between the optical and THz pulses. A nonlinear polarization is generated via optical rectification in the PPLN, and each domain in the PPLN contributes a half-cycle to the radiated THz field. In the absence of absorption and domain length fluctuations, the relative bandwidth of the THz field is simply $\Delta\nu/\nu = N/2$, where N is the number of domains in the crystal. The THz wave is generated with the frequency of $\nu = c/2l_d(n_{\text{opt}} - n_{\text{THz}})$ where l_d is domain width, and n_{opt} and n_{THz} are the group refractive indices at optical and THz frequencies, respectively.¹⁰ Since the THz frequency is determined only by the domain width and the relevant indices of refraction, frequency tuning can be easily accomplished by varying the domain width.

Because of the large material absorption coefficient at THz frequencies, however, the bandwidth and power of the THz wave from the PPLN are severely hampered at room temperature. The main source of the absorption is the low frequency tail of the transverse optical (TO) phonon mode at 7.6 THz, although additional low-frequency resonances have been observed and may contribute.^{11,12} The mechanisms of the THz loss have been investigated recently;^{11,13,14} the TO phonon polaritons can decay by coupling to two acoustic phonons and by scattering at crystal defects. The TO coupling to low-frequency modes is weaker at low temperatures, resulting in smaller THz absorption. Qiu and Maier¹⁴ have also observed coupling to a Debye relaxational mode at room temperature which is not present at liquid nitrogen temperatures. Shikata and co-workers have previously demonstrated that the absorption of THz waves in lithium niobate is suppressed substantially at low temperature.⁹ Thus, cooling of the PPLN crystal should be expected to reduce strongly the THz absorption. In this letter, we demonstrate narrow-band THz generation from PPLN crystals at low temperature, and discuss the temperature dependence of the THz absorption and power. We measure the absolute power of the THz emission for various pump conditions using a bolometer, and calculate the optical to THz conversion efficiency.

The samples used in the experiments reported here were 1.2 and 7.2 mm z -cut PPLN crystals with domain width $l_d = 30 \mu\text{m}$. The sample height and width were 0.5 and 6.5 mm, respectively. Optical pump pulses of 200 fs duration at 800 nm from a 250 kHz Ti:sapphire regenerative amplifier¹⁵ were used for the THz generation. The incident optical pump was focused to a roughly $100 \mu\text{m}$ spot in the crystal, and the power was varied from 20 to 500 mW. For wave form measurements, the radiated THz wave was collimated with an off-axis paraboloid and focused into a 1 mm ZnTe crystal for electro-optic detection of the THz field.¹⁶ The excitation beam was acousto-optically modulated at 50 kHz for lock-in signal detection. For the THz power measurement, a bolometer with a silicon detector kept at liquid helium temperature was used. The samples were mounted on the cold finger of a cryostat and the temperature was varied from 18 to 298 K.

^{a)}Electronic mail: yunslee@eecs.umich.edu

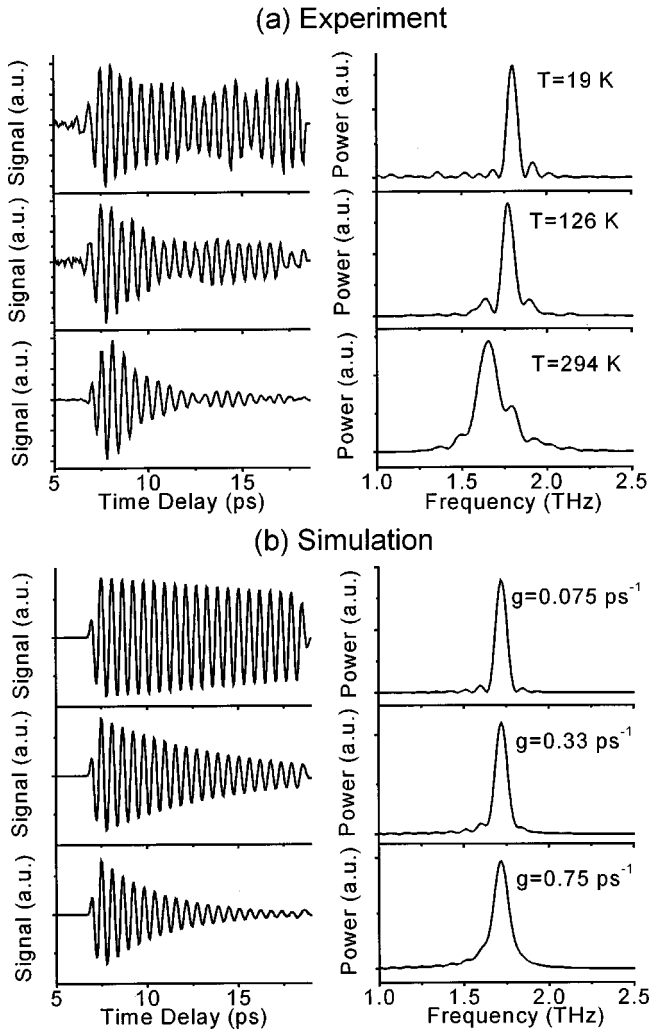


FIG. 1. THz wave forms and power spectra of (a) the experimental results at $T=19$, 126, and 298 K, and (b) the simulation results for $g=0.075$, 0.33, and 0.75 ps from the 1.2 mm PPLN crystal.

Figure 1(a) shows the measured THz wave forms and power spectra at $T=19$, 126, and 298 K from the 1.2 mm PPLN sample. At low temperature, the wave form consists of 20 cycles of relatively equal amplitude; this corresponds to the 20 periods of the PPLN domain structure. On the other hand, a strong temporal decay of the wave form due to THz absorption is observed at room temperature, which results in a substantial broadening of the THz spectrum. The bandwidths of the spectra are 0.071, 0.081, and 0.14 THz at $T=18$, 126, and 298 K, respectively. The broadening is approximately constant for temperatures below about 120 K, although the THz power increases substantially as the temperature decreases. It is also observed that the spectrum shifts to the red with increasing temperature. The spectral center is located at 1.81, 1.77, and 1.65 THz for $T=19$, 126, and 198 K. The frequency shift is due to an interplay of the temperature-dependent index of refraction and the thermal expansion (which causes the domain width to increase as temperature rises, and the THz frequency is inversely proportional to the PPLN domain width).¹⁰

In order to model the THz generation, the wave equations are solved with a nonlinear source term.¹⁰ At the exit surface of the crystal ($z=L$), the contribution of the THz field from position z' is

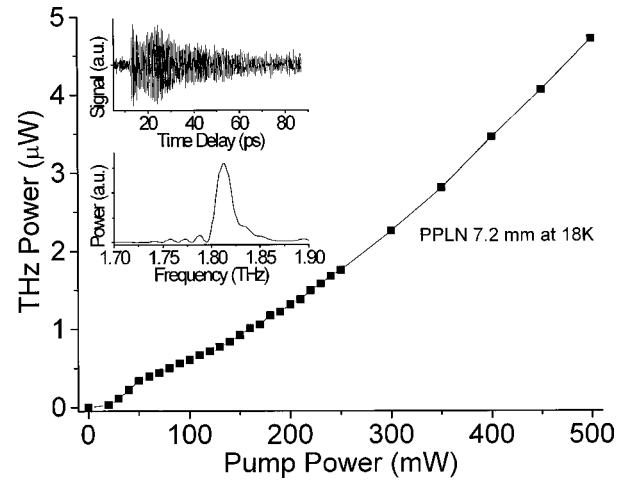


FIG. 2. THz power from the 7.2 mm PPLN crystal at $T=18$ K vs optical pump power at 800 nm. THz wave form and power spectrum for $I_p=200$ mW are shown in the inset.

$$E_{\text{THz}}^{\text{local}}(z', t) = \frac{\pm A_0 \tau}{4 \left\{ \frac{\tau^2}{4} + \frac{g}{c} (L - z') \right\}^{3/2}} \times \left[\frac{[t - t_d(z')]^2}{2 \left\{ \frac{\tau^2}{4} + \frac{g}{c} (L - z') \right\}} - 1 \right] \times \exp \left[- \frac{[t - t_d(z')]^2}{2 \left\{ \frac{\tau^2}{4} + \frac{g}{c} (L - z') \right\}} \right], \quad (1)$$

where $t_d(z') = [n_{\text{opt}} z' + n_{\text{THz}} (L - z')] / c$. The temporal evolution of the THz wave is obtained by integrating the electric field in the spatial domain over the crystal length. The imaginary part of the THz index of refraction is assumed to be $\kappa_{\text{THz}} = g\omega$.^{9,10} In Fig. 1(b), the simulated wave forms and power spectra are shown. The THz absorption and spectral broadening are well reproduced in the simulation. The bandwidths of the spectra are 0.086, 0.081, and 0.12 THz for $g=0.075$, 0.33, and 0.75 ps. As in the experimental results, the bandwidth broadening is not significant until g is larger than 0.33 ps. Since the temperature dependence of the refractive indices and domain width are not included, the spectral shift is not reproduced in the calculation. The experimental results show more structure in the wave form and a broader bandwidth than the simulation results because of domain structure fluctuations and the presence of coherent THz reradiation arising from resonances in the PPLN sample. A discussion of these phenomena will be presented elsewhere.

Absolute power measurements were made using a liquid helium bolometer. Since the emitted power increases with crystal length (in the absence of absorption), we used the 7.2 mm sample for the power measurements. Figure 2 shows the detected THz power versus optical pump power (I_p) at $T=18$ K. A variable attenuator controlled the pump power. Below 50 mW of pump power, the THz power is proportional to I_p^2 as expected for optical rectification, but at higher pump power, the exponent is reduced to 1.55. We believe the reason for this to be that since lithium niobate is a photorefractive material, there is an increased absorption and scat-

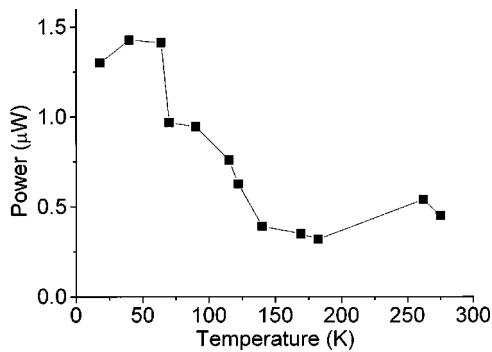


FIG. 3. THz power from the 7.2 mm PPLN crystal vs temperature for $I_p = 200$ mW.

tering due to photorefraction at low temperature. The maximum power obtained is about $5 \mu\text{W}$, corresponding to an average power of 0.3 W over the THz pulse duration. The power and photon conversion efficiencies are about 10^{-5} and 2×10^{-3} at $I_p = 500$ mW, respectively. The spectral density of the THz source is thus 2.8×10^{-4} W/THz. This should be compared with single-cycle THz generation from velocity-matched optical rectification in ZnTe, from which we have also observed $5 \mu\text{W}$ of power just below the damage threshold of the crystal (≈ 250 mW). In that case we find a spectral density at 1.8 THz of 1.7×10^{-6} W/THz.

The THz wave form and power spectrum at $I_p = 200$ mW are shown in the inset of Fig. 2. The decay time is about 50 ps which corresponds to $g = 0.075$ ps. The bandwidth of the 7.2 mm PPLN crystal is 0.018 THz which is a factor of 4 smaller than for the 1.2 mm PPLN crystal. According to the simulation including absorption, the ideal bandwidth of the 7.2 mm PPLN is 0.011 THz. The broader bandwidth of the experimental wave form indicates that the primary factor limiting the bandwidth in the long crystal is fluctuations of the domain width, which may be thought of as a kind of “inhomogeneous broadening” of the THz emission.

The temperature dependence of the THz power from the 7.2 mm crystal at a fixed optical pump power of 200 mW is shown in Fig. 3. In this case, the power is computed from the measured wave form, and is calibrated to the bolometric

measurement at low temperature. The THz power decreases nearly monotonously as temperature increases to about 120 K. Above this temperature, there is very little decrease in emitted power. Note that operation at liquid nitrogen temperature gives a substantial benefit in power and bandwidth; operation at liquid helium temperature will not be necessary for most applications.

In summary, we have shown that the bandwidth and power of THz generated by optical rectification in PPLN at room temperature is limited by THz absorption in the crystal. Since the losses due to TO phonon absorption are strongly reduced at low temperature, substantially larger power and narrower bandwidth are obtained by cooling the crystal. We have generated up to $5 \mu\text{W}$ of power at 1.8 THz in a bandwidth of only 18 GHz, which we expect will make this a significant source of coherent THz radiation for applications where spectral density is important.

This work was supported by ARO under Grant No. DAAH04-96-1-0414 and by NSF under Grant No. DMR-9729109. The authors thank Phil Bucksbaum for loan of the bolometer.

¹F. Zernike, Jr. and P. R. Berman, Phys. Rev. Lett. **15**, 999 (1965).

²R. Morris and Y. R. Shen, Phys. Rev. A **15**, 1143 (1977).

³K. Kawase, M. Mizuno, S. Sohma, H. Takahashi, T. Taniuchi, Y. Urata, S. Wada, H. Tashiro, and H. Ito, Opt. Lett. **24**, 1065 (1999).

⁴E. R. Brown, K. A. McIntosh, K. B. Nichols, and C. L. Dennis, Appl. Phys. Lett. **66**, 285 (1995).

⁵S. Matsuura, M. Tani, and K. Sakai, Appl. Phys. Lett. **70**, 559 (1997).

⁶A. Nahata, J. T. Yardley, and T. F. Heinz, Appl. Phys. Lett. **75**, 2524 (1999).

⁷K. Kawase, M. Sato, T. Taniuchi, and H. Ito, Appl. Phys. Lett. **68**, 2483 (1996).

⁸K. Kawase, M. Sato, K. Nakamura, T. Taniuchi, and H. Ito, Appl. Phys. Lett. **71**, 753 (1997).

⁹J. Shikata, M. Sato, T. Taniuchi, and H. Ito, Opt. Lett. **24**, 202 (1999).

¹⁰Y.-S. Lee, T. Meade, V. Perlin, H. Winful, T. B. Norris, and A. Galvanuskas, Appl. Phys. Lett. **76**, 2505 (2000).

¹¹U. T. Schwartz and M. Maier, Phys. Rev. B **53**, 5074 (1996).

¹²H. J. Bakker, S. Hunsche, and H. Kurz, Phys. Rev. B **50**, 914 (1994).

¹³G. P. Wiederrecht, T. P. Dougherty, L. Dhar, K. A. Nelson, D. E. Leaird, and A. M. Weiner, Phys. Rev. B **51**, 916 (1995).

¹⁴T. Qiu and M. Maier, Phys. Rev. B **56**, R5717 (1997).

¹⁵T. B. Norris, Opt. Lett. **17**, 1009 (1992).

¹⁶Q. Wu and X.-C. Zhang, Appl. Phys. Lett. **68**, 1604 (1996).